Synthesis and Molecular Modeling of 1-Phenyl-1,2,3,4-tetrahydroisoquinolines and Related 5,6,8,9-Tetrahydro-13b*H*-dibenzo[*a*,*h*]quinolizines as D_1 Dopamine Antagonists

Deborah L. Minor,[†,#] Steven D. Wyrick,[*,†] Paul S. Charifson,[†,@] Val J. Watts,[‡,§] David E. Nichols,[⊥] and Richard B. Mailman[†,‡,§,∥]

Division of Medicinal Chemistry and Natural Products, School of Pharmacy, Brain and Development Research Center, Departments of Psychiatry and Pharmacology, School of Medicine, University of North Carolina, Chapel Hill, North Carolina 27599-7360, and Department of Medicinal Chemistry and Pharmacognosy, School of Pharmacy, Purdue University, West Lafayette, Indiana

Received June 27, 1994[⊗]

New 1-phenyl-1,2,3,4-tetrahydroisoquinolines and related 5,6,8,9-tetrahydro-13b*H*-dibenzo[*a*,*h*]-quinolizines were prepared as ring-contracted analogs of the prototypical 1-phenyl-2,3,4,5-tetrahydrobenzazepines (e.g., SCH23390) as a continuation of our studies to characterize the antagonist binding pharmacophore of the D_1 dopamine receptor. Receptor affinity was assessed by competition for [^{3}H]SCH23390 binding sites in rat striatal membranes. The 6-bromo-1-phenyltetrahydroisoquinoline analog **2** of SCH23390 **1** had D_1 binding affinity similar to that for the previously reported 6-chloro analog **6**, whereas the 6,7-dihydroxy analog **5** had significantly lower D_1 affinity. Conversely, neither 6-monohydroxy- (**3**) nor 7-monohydroxy–1-phenyltetrahydroisoquinolines (**4**) had significant affinity for the D_1 receptor. These results demonstrate that 6-halo and 7-hydroxy substituents influence D_1 binding affinity of the 1-phenyltetrahydroisoquinolines in a fashion similar to their effects on 1-phenyltetrahydrobenzazepines. The conformationally constrained 3-chloro-2-hydroxytetrahydrodibenzoquinolizine **9** had much lower affinity relative to the corresponding, and more flexible, 6-chloro-7-hydroxy-1-phenyltetrahydroisoquinoline **6**. Similarly, 2,3-dihydroxytetrahydrodibenzoquinolizine **10** had much lower D_1 affinity compared to dihydrexidine **14**, a structurally similar hexahydrobenzo-[*a*]phenanthridine that is a high-affinity full D_1 agonist. Together, these data not only confirm the effects of the halo and hydroxy substitutents on the parent nucleus but demonstrate the pharmacophoric importance of both the nitrogen position and the orientation of the accessory phenyl ring in modulating D_1 receptor affinity and function. Molecular modeling studies and conformational analyses were conducted using the data from these new analogs in combination with the data from compounds previously synthesized. The resulting geometries were used to refine a working model of the D_1 antagonist pharmacophore using conventional quantitative structure–activity relationships and three–dimensional QSAR (CoMFA).

Introduction

Dopamine neurotransmission plays a major role in the etiology and/or therapy of a variety of neurological and psychiatric disorders, including Parkinson's disease, schizophrenia, Huntington's disease, and others.[1] Thus, there are compelling reasons to understand the molecular pharmacology of dopamine receptors. More than a decade ago, the existence of two dopamine receptor subtypes, D_1 and D_2, was proposed.[2,3] For several years afterward, it was believed that the important clinical actions of dopamine receptor ligands (e.g., antagonists like the antipsychotic drugs or agonists used to treat Parkinson's disease) were primarily mediated by the D_2 class of receptor.[4–6] This viewpoint was due, in large measure, to the lack of appropriate pharmacological probes for the D_1 receptor. Thus, a major breakthrough occurred when the first high-affinity and selective D_1 antagonist SCH23390 (**1**, Figure 1) became available,[7] leading to awareness of important roles for D_1 receptors in a host of CNS-mediated functions, alone and via interactions with D_2 receptors.[8–11]

It is now known that at least five genes code for dopamine receptor isoforms, with the isoforms often divided into subfamilies called "D_1-like" and "D_2-like".[12] Two of these isoforms, termed D_{1A}[13–16] and D_5[17] (or D_{1B}[18]), have a high degree of molecular homology and share similar D_1-like pharmacology. The important functional roles for D_1-like receptors were heightened recently by studies reporting a critical role for full (but not partial) activation of D_1 receptors in the pharmacotherapy of parkinsonism.[19] Such data underscore the importance of understanding the mechanisms affecting drug recognition and activation (or antagonism) at the D_1 receptor.

We previously synthesized a series of 1-phenyl-1,2,3,4-tetrahydroisoquinoline analogs[20] that were ring-contracted analogs of the 1-phenyl-2,3,4,5-tetrahydrobenzazepine **1** and reported conformational analysis studies[21] utilizing molecular mechanics calculations on both series. Results indicated that the lowest energy con-

* Person to whom correspondance should be addressed.
† Division of Medicinal Chemistry and Natural Products, School of Pharmacy, University of North Carolina.
‡ Brain and Development Research Center, University of North Carolina.
§ Departments of Psychiatry and Pharmacology, University of North Carolina.
∥ School of Medicine, University of North Carolina.
⊥ Department of Medicinal Chemistry and Phamacognosy, Purdue University.
@ Current address: Glaxo, Inc., Five Moore Dr., Research Triangle Park, NC 27709.
# Current address: Molecular Simulations, Inc., 3724 Durham Highway, Raleigh, NC 27614.
⊗ Abstract published in *Advance ACS Abstracts*, November 1, 1994.

0022-2623/94/1837-4317$04.50/0

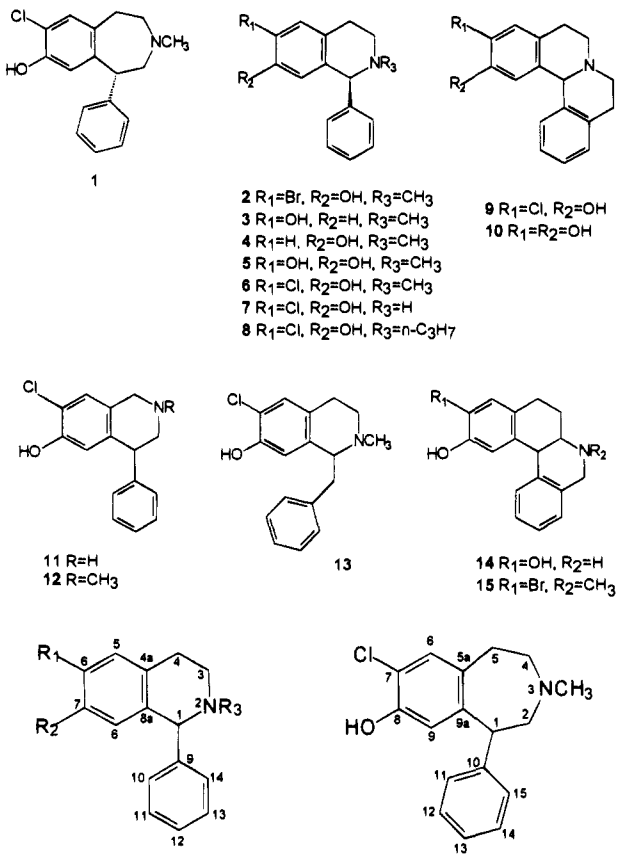

Figure 1. Structural analogs used for D_1 receptor studies. (Torsion angle, τ, is defined by 8a, 1, 9, 10 or 9a, 1, 10, 11.)

formation for the 1-phenyltetrahydroisoquinolines is that in which the heterocyclic ring exists in a half-chair conformation with an equatorial *N*-substituent and pseudoequatorial accessory phenyl ring held in a nearly orthogonal orientation relative to the fused ring system. On the other hand, the lowest energy 1-phenyltetrahydrobenzazepine conformation is that in which the heterocyclic ring exists in a chair conformation with an equatorial *N*-substituent and an equatorial accessory phenyl ring.

Studies performed by Pettersson *et al.*[22] on 1-phenyltetrahydrobenzazepines and some constrained analogs led to similar findings. They have calculated electrostatic potentials of various 1-phenyltetrahydrobenzazepine D_1 ligands and suggested that a large degree of the interaction between the accessory phenyl ring and the receptor is electrostatic in nature and that the phenyl ring interacts with the same site on the receptor as does the 8-hydroxyl group. A report by Weinstock[24] suggests that conformationally flexible 1-phenyltetrahydrobenzazepines may prefer to attain an axial accessory phenyl ring conformation in order to bind to the D_1 receptor, whereas the equatorial conformation may be favored for access to the binding site.

We reported the development of a quantitative structure–activity relationship (QSAR) model for D_1 dopamine receptor antagonists of the 1-phenyltetrahydroisoquinoline and 1-phenyltetrahydrobenzazepine series.[21] The key regressor utilized, cosine θ, represented a combined steric and electronic parameter based upon the orientation of the net molecular dipole relative to the three-dimensional arrangement of the pharmacophoric elements for a given set of 1-phenyltetrahydroisoquinoline derivatives and **1**. It was revealed by this model that, at the D_1 receptor, the active 1-phenyltetrahydroisoquinolines (*S* absolute configuration) have opposite stereochemical requirements to the 1-phenyltetrahydrobenzazepines. It was also shown that these two classes share common structure–activity relationships, such as the sensitivity of antagonist binding affinity to the nature of the *N*-substituent and nitrogen lone electron pair (or N^+H for the protonated species) vector orientation. More specifically, the corresponding *N*-normethyl derivative **7** of *(S)*-(+)-6-chloro-7-hydroxy-1-phenyl-*N*-methyl-1,2,3,4-tetrahydroisoquinoline (**6**) (Figure 1) demonstrated approximately 17 times less affinity as a D_1 ligand relative to the *N*-methyl analog. Similarly, **1** was twice as potent in binding to the D_1 receptor as its *N*-normethyl derivative.

The present work reports the synthesis of additional 1-phenyltetrahydroisoquinolines and related analogs (Figure 1, Schemes 1 and 2) and the use of these compounds to extend molecular modeling studies of D_1 receptor antagonists. Since **1** and **6** both have significant affinity as selective D_1 antagonists, they were utilized as templates for comparison of the compounds reported herein. Compounds **3** and **4** (Figure 1) were designed to investigate the significance of the halogen in the aromatic 6-position of the 1-phenyltetrahydroisoquinoline versus the 7-halo substituent in the 1-phenyltetrahydrobenzazepine series. Analog **5**, a catechol, was synthesized to determine whether this compound would have partial agonist properties as are seen with SKF38393, a tetrahydrobenzazepine that lacks the *N*-methyl group.

As noted above, earlier molecular modeling and NMR data have led to the hypothesis that the accessory phenyl ring in the 1-phenyltetrahydroisoquinoline and 1-phenyltetrahydrobenzazepine series prefers a nearly orthogonal orientation with energy minima corresponding to torsion angle τ(8a,1,9,10 or 9a,1,10,11, Figure 1) at approximately 60° and 90°, respectively, to the fused ring systems.[21] For this reason, it was predicted that this phenyl ring orientation might be one important criterion for D_1 receptor antagonist versus agonist binding affinity. To test this hypothesis, the 3-chloro-2-hydroxy-5,6,8,9-tetrahydro-13b*H*-dibenzo[*a*,*h*]quinolizine analog **9** was prepared since it contains the analogous accessory phenyl ring constrained in a less orthogonal orientation (analogous torsion angle ca. 12°) relative to the fused ring system. It was hypothesized that such a change would decrease affinity. The tetrahydrodibenzoquinolizine **10**, a compound structurally similar to the full D_1 agonist dihydrexidine (**14**),[25,26] was designed to investigate the importance of the nitrogen position for D_1 antagonist versus agonist properties. The nitrogen in **14** is at an adjacent position to the nitrogen in **10**. Analog **15**, a low-affinity D_1 antagonist derivative of **14** in which one of the catechol hydroxyls is replaced by a bromine and the secondary nitrogen of **14** is methylated, also was included.[25,26] This analog incorporates the proposed accessory phenyl ring orientation of an agonist, but also the tetrahydroisoquinoline aryl substitution pattern and nitrogen substitution pattern of an antagonist. This mixed agonist–antagonist pharmacophoric arrangement probably accounts for the low affinity reported for **15**.

Scheme 1

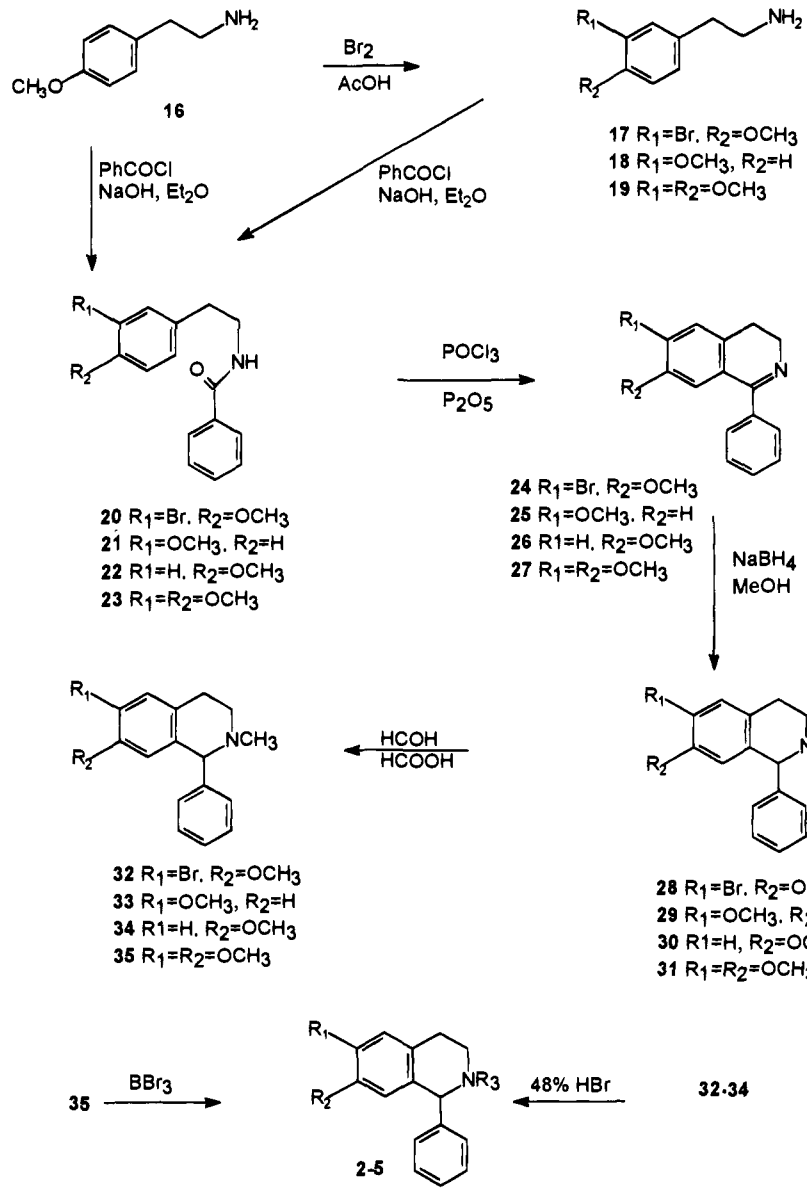

Scheme 2

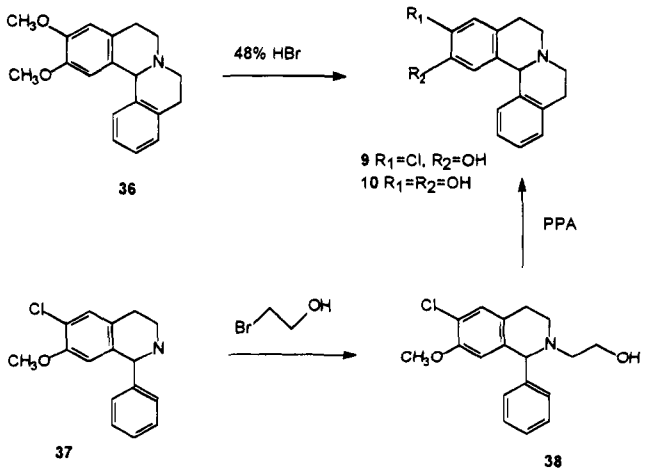

The modeling techniques employed in these studies include modification of our previous QSAR model[21] as well as comparative molecular field analysis (CoMFA), a recently developed method by Kramer et al.[27] that correlates the steric and electrostatic fields of molecules with biological activity. In addition, the previously reported "Active Analogue Approach"[21] was extended by inclusion of the additional 1-phenyltetrahydroisoquinolines, tetrahydrodibenzoquinolizines, and hexahydrobenzophenanthridines. These additional classes were used to refine that volume and shape of the D_1 receptor that is able to accommodate the active ligands and, conversely, that volume partially occupied by the receptor itself that excludes the inactive analogs.

Chemistry

Schemes 1 and 2 outline the synthesis of the target compounds **2–5** and **9–10**. The additional 1-phenyltetrahydroisoquinolines included herein were prepared by the procedure previously reported.[20] Briefly, the phenethylamine intermediates **16–19** were reacted with benzoyl chloride to afford the respective benzamides **20–23** that were then ring-closed via a Bischler–Napieralski cyclization[28] to afford the 3,4-dihydroisoquinolines (**24–27**). This was followed by reduction of the imine utilizing sodium borohydride to afford **28–**

Table 1. 1-Phenyltetrahydroisoquinolines and Synthetic Intermediates

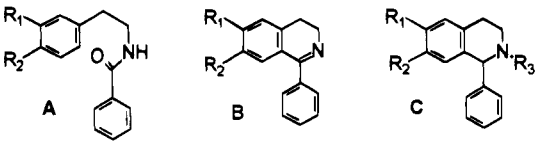

compd no.	compd type	R_1	R_2	R_3	mp °C	% yield	recrystn/eluting solvent	formula	analyses
20	A	Br	OCH_3		gum	83	*a*	$C_{16}H_{16}BrNO$	
21	A	OCH_3	H		67	57	*a*	$C_{16}H_{17}NO_2$	
22	A	H	OCH_3		121	78	*a*	$C_{16}H_{17}NO_2$	
23	A	OCH_3	OCH_3		85–86	85	*a*	$C_{17}H_{19}NO_3$	
24	B	Br	OCH3		gum	14	Hex/EtOAC[c]	$C_{16}H_{14}BrNO$	
25	B	OCH_3	H		gum	38	*a*	$C_{16}H_{15}NO$	
26	B	H	OCH_3		gum	5	Hex/EtOAC[c]	$C_{16}H_{15}NO$	
27	B	OCH_3	OCh_3		211–213	72	Hex/Tol[c]	$C_{17}H_{17}NO_2$	
28	C	Br	OCH_3	H	107–108	57	Hex/EtOAC[b]	$C_{16}H_{16}BrNO_2$	
29	C	OCH_3	H	H	73–74	67	*a*	$C_{16}H_{17}BrNO$	
30	C	H	OCH_3	H	74–75	66	*a*	$C_{16}H_{17}BrNO$	
31	C	OCH_3	OCH_3	H	102–103	74	Hex/EtOAC[c]	$C_{16}H_{19}NO_2$	
32	C	Br	OCH_3	CH_3	73–74	86	Hex/EtOAC[c]	$C_{17}H_{18}BrNO$	
33	C	OCH_3	H	CH_3	63–64	20	Hex/EtOAC[c]	$C_{17}H_{19}NO$	
34	C	H	OCH_3	CH_3	76–78	39	*a*	$C_{17}H_{19}NO$	
35	C	OCH_3	OCH_3	CH_3	77–78	91	*a*	$C_{18}H_{21}NO_2$	
2	C	Br	OH	CH_3	178–179	13	Hex/EtOAC[b]	$C_{16}H_{16}BrNO$	C,H,N
3	C	OH	H	CH_3	185–187	89	Hex/EtOAC[b]	$C_{16}H_{17}NO$	C,H,N
4	C	H	OH	CH_3	184–186	83	Hex/EtOAC[b]	$C_{16}H_{17}BrNO_2$	C,H,N
5	C	OH	OH	CH_3	>350	25	*a*	$C_{16}H_{17}NO_2$	C,H,N

[a] No purification was necessary. [b] Recrystallization solvent. [c] Eluting solvent for column chromatography.

31. Methylation of the nitrogen was carried out by the Eschwieler–Clark *N*-methylation procedure[29] to afford **32**–**35**. Finally, cleavage of the methoxy groups was achieved with either hydrobromic acid[30] to afford analogs **2**–**4** or boron tribromide to afford analog **5**.

Scheme 2 indicates the synthesis of the dibenzoquinolizine analogs **9** and **10**. The nitrogen of **37** was initially alkylated with bromoethanol to afford **38** followed by subsequent ring closure and *O*-demethylation utilizing polyphosphoric acid to afford **9**. The synthesis of **10** was accomplished by the *O*-demethylation of **36**[31] using 48% hydrobromic acid.

The method described by Gold and Chang[30] for similarly substituted 1-phenyltetrahydrobenzazepines was used for the enantiomeric resolution of the racemic intermediate **28**. Racemic **28** was converted to the diastereomeric salts using *N*-acetyl-D-leucine, with consecutive recrystallizations in acetonitrile yielding the (+)-diastereomer. The filtrates were then converted to the free base followed by conversion to the diastereomeric salts using *N*-acetyl-L-leucine. Consecutive recrystallizations in acetonitrile afforded the (−)-diastereomer. Both the (+)- and (−)-diastereomers were converted to the free base enantiomers using 5% NaOH solution. Each enantiomer was converted to the *N*-methylated derivative using formaldehyde and formic acid, accompanied by a reversal in the sign of rotation. The *N*-methylated derivatives were then *O*-demethylated in the presence of 48% hydrobromic acid to afford (*S*)-(+)- and (*R*)-(−)-**2**. After catalytic dehalogenation of (−)-**2** and (−)-**6** in the presence of H_2/Pd/C in THF, the absolute configuration of (−)-**2** was determined by comparison of the sign of rotation to that of (*R*)-(−)-**4**.

Results and Discussion

We previously reported that a series of 1-phenyltetrahydroisoquinolines had affinity for the D_1 receptor[20] when compared to the prototypical antagonist 1. Upon the expansion of these SAR studies with additional related analogs (**2**, **3**, **4**, **5**, **9**, **10**, **15**), a broad range of affinities for the D_1 receptor, concomitant with little D_2 affinity, was demonstrated (Table 2). Compounds **3** and **4** demonstrated little affinity for the D_1 receptor at the concentration range used in the competition study (Table 2), suggesting that the halogen and the hydroxyl substituents in the **6**- and **7**-positions, respectively, were necessary. Pettersson et al.[23] have hypothesized that the accessory phenyl ring in the 1-phenyltetrahydrobenzazepines interacts with the same site on the receptor as does the 8-hydroxyl group. Although there are other explanations for this, it is not surprising that the 1-phenyltetrahydroisoquinoline **3** (lacking the analogous hydroxyl) was found to be inactive. Binding affinity for the bromo analog **2** was comparable to that for the remaining two prototypes in this study (1 and **6**; Table 2), suggesting that the receptor domain that accommodates the chlorine atom has tolerance for larger halogens, similar to the pattern seen with other D_1 antagonists such as 1. Since the active enantiomer for **2** possesses the *S* absolute configuration, it appears that the sterochemical requirement for this compound is analogous to that of the chloro analog **6** with regard to affinity and selectivity. As noted earlier, it was anticipated that the catechol analog **5** might have agonist-like binding characteristics; D_1 antagonists typically have Hill slopes equal to 1, but significantly less than 1.0 for agonists. The Hill slope for **5** was, in fact, 0.913, suggesting that this compound would, at best be only a partial agonist. As expected, there was no significant correlation ($r = 0.155$) between D_1 and D_2 binding affinity for the test compounds included in this study.

On the basis of previous NMR and molecular modeling studies as well as X-ray crystallographic data,[21] it was determined that the accessory phenyl ring in the 1-phenyltetrahydroisoquinoline and 1-phenylbenzazepine antagonists is held in a nearly orthogonal

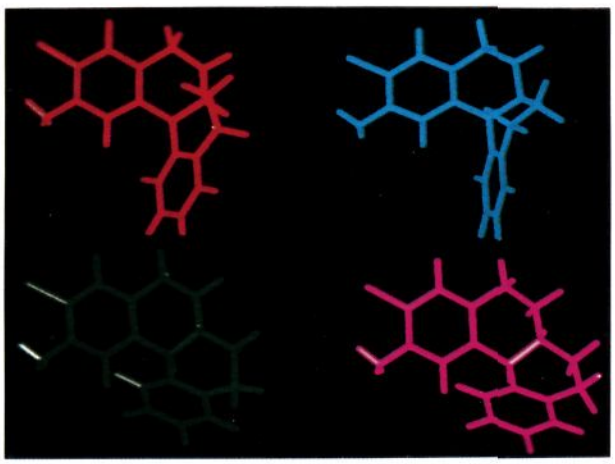

Figure 2. Four lowest energy conformations for **9**. *N*-Axial chair, chair (red); *N*-axial chair, boat (blue); *N*-equatorial chair, chair (green); *N*-equatorial chair, boat (magenta).

orientation relative to the fused ring system. Although the *(S)*-tetrahydroisoquinolines superimposed well upon the lowest energy conformation of *(R)*-**1**, we found that another low-energy conformation of **1**, a twist chair of 1.56 kcal/mol higher energy compared to the global minimum energy conformation, better correlated with the tetrahydroisoquinolines and other analogs in the conventional and CoMFA QSAR models presented herein. This conformation, when used as the template in the Multifit analysis described below, also resulted in lower energy multifit or "pharmacophoric" conformations for the series as compared to those that resulted when the lowest energy conformation of **1** was used. These results suggest that this may represent a more probable conformation of **1** for receptor binding. The twist chair conformation of **1** also involves the phenyl ring held in a similar orthogonal orientation. This led us to hypothesize that the accessory phenyl ring orientation was important in distinguishing agonist from antagonist binding potential for the D_1 receptor.

For this reason, we proposed the synthesis of the dibenzoquinolizine analog **9** in which the ring is constrained in a less orthogonal orientation. As expected, **9** demonstrated significantly reduced binding affinity as compared to the corresponding more flexible analog **6**, suggesting the necessity of this ring orientation for D_1 antagonist affinity. Molecular mechanics-based conformational analysis indicated that one of the four lowest energy conformations of **9** (Figure 2) is that in which the ethano bridge from the nitrogen to the accessory ring is in the equatorial position on the nitrogen, with the two heterocyclic rings in a half-chair conformation allowing the corresponding accessory phenyl ring to exist in a less orthogonal orientation relative to the tetrahydroisoquinoline ring system. ^{1}H-NMR data for the 1-phenyltetrahydroisoquinolines and 1-phenyltetrahydrobenzazepines (possessing the nonconstrained ring) reveals that the proton in the 8-position and corresponding 9-position, respectively, is shifted substantially upfield in comparison to the remaining aromatic protons, probably due to the shielding effect produced by the orthogonal phenyl ring. No such NMR shielding was exhibited for **9**, however, indicating that the phenyl ring must be in a non-orthogonal orientation. Therefore, of the four lowest energy conformations for **9**, NMR data eliminated the possibility of the two *N*-axial forms in which the accessory ring is held orthogonally. Consequently, the lowest energy conformer of the remaining two structures (the *N*-equatorial half-chair, half-chair conformation) (3.66 kcal/mol) was chosen as the most plausable conformation for this tetrahydrodibenzoquinolizine to be used in subsequent modeling and QSAR studies. Likewise, the low-affinity hexahydrobenzophenanthridine D_1 antagonist[25] analog **15** possesses the corresponding phenyl ring constrained in a less orthogonal orientation.

The catechol-type tetrahydrodibenzoquinolizine **10** was prepared to investigate the importance of the nitrogen position for D_1 agonist versus antagonist affinity. This compound is structurally and conformationally similar to the potent, full D_1 agonist dihydrexidine (**14**),[25] differing only in the position of the ring nitrogen. The affinity of **10** for the D_1 receptor (Table 2) was 270-fold less than that of **14** (IC50 10 ± 1 nM) suggesting the importance of the nitrogen position as a component of the D_1 agonist versus antagonist pharmacophore. It should be noted that the present studies included neither **14** nor other D_1 agonists in the modeling work described herein. This decision was based on the assumption that there are important differences in certain aspects of the modes of binding that occur with agonists versus antagonists. In fact, most D_1 agonists based on the phenyltetrahydrobenzazepine (e.g., SKF38393) are partial agonists that clearly have both agonist and antagonist characteristics. An understanding of the molecular characteristics of the antagonist pharmacophore is a necessary foundation for investigation of the more complicated situation with mixed agonists–antagonists.

Conventional Regression Analysis (QSAR)

As stated above, we previously developed a QSAR model for a limited series of 1-phenyltetrahydroisoquinolines and **1** as D_1 dopamine receptor antagonists ($r^2 = 0.902$).[21] To develop this model, a special angular regressor, cosine θ, was developed and defined as the angle between the molecular dipole moment vector and the normal to the pharmacophoric plane through the center of mass. Atoms designated as pharmacophoric elements included the cationic nitrogen, 6-chloro, 7-hydroxyl, and the centroid of the accessory phenyl ring. The analogous elements were utilized for **1**. Incorporation of cosine θ values for the additional compounds described in this study into the original parabolic model resulted in a dramatic decrease in the correlation coefficient ($r^2 = 0.216$; Table 3), indicating the limitations of this model. For the seven compounds included in the original model, the torsion angle τ(a,b,c,d) defining the orientation of the accessory phenyl ring was similar for all observations in the data set with the exception of a 1-benzyltetrahydroisoquinoline analog for which the analogous torsion angle could not be defined. When the tetrahydrodibenzoquinolizines (τ(a,b,c,d) approximately 12°) were included, this model failed to describe sufficiently the steric aspects of the observations. Subsequently, univariate linear regression using the expanded set of analogs with cosine θ as a descriptor also afforded a similarly inadequate correlation ($r^2 = 0.216$) (Table 3). The correlation was greatly enhanced ($r^2 = 0.916$, Tables 3 and 4) by incorporating the torsion

Table 2. D_1 and D_2 Receptor Affinities

compd no.	K_iD_1[a]	pK_iD_1	K_iD_2[b]	pK_iD_2	D_1 selectivity D_2/D_1
(*R*)-(+)-**1**	0.40 ± 0.09	9.39	676 ± 38	6.17	1690
(*S*)-(+)-**2**	8.30 ± 2.3	8.08	1300 ± 190	5.88	156.6
(*R*)-(−)-**2**	>5000	*c*	>5000	*c*	*c*
(+)-**3**	>5000	*c*	>5000	*c*	*c*
(±)-**4**	>5000	*c*	>5000	*c*	*c*
(±)-**5**	370 ± 82	6.73	290 ± 36	6.53	1.27
(*S*)-(+)-**6**	6.6 ± 0.7	8.04	1850 ± 240	5.73	205.5
(*R*)-(−)-**6**	442 ± 27	6.35	19200 ± 430	4.71	43.4
(±)-**7**	743 ± 76	6.85	26300 ± 1300	5.43	35.39
(±)-**8**	179 ± 5	6.75	1900 ± 100	5.72	10.6
(±)-**9**	830 ± 44	6.38	>5000	*c*	*c*
(±)-**10**	2700 ± 400	5.86	>5000	*c*	*c*
(±)-**11**	565 ± 61	6.55	3620 ± 600	5.44	6.40
(±)-**12**	174 ± 17	6.75	522 ± 108	6.28	3.0
(±)-**13**	53.2 ± 4.0	7.27	287 ± 32	6.54	5.39
(±)-**15**	138 ± 44	6.85	>3000	*c*	*c*

[a] D_1 potency was determined from competition binding with [^{3}H]SCH23390.[1] All values expressed as a mean K_i (nM) value + SEM. [b] D_2 potency was determined from competition binding with [^{3}H]spiperone. All values expressed as a mean K_i (nM) value + SEM. [c] Finite values could not be calculated.

Table 3. Statistical Results from Conventional QSAR

compd[a]	regressor	analysis	R	R^2	F	SE	p
A	cos θ	PN[b]	0.950	0.902	18.445	0.384	0.009
A + B	cos θ	PN	0.465	0.216	1.213	0.988	0.372
A + B	cos θ	univariate linear linear multiple	0.464	0.216	2.749	0.938	0.128
A + B*	cos θ, τ^c	multiple	0.957	0.916	43.575	0.324	0.0001

[a] A = **1** + **6** + **7** + **8** + **11** + **12** + **13**. B = **2** + **5** + **9** + **10** + **15**. B* = All compounds except **13**. [b] PN = polynomial. [c] τ = torsion angle 8a, 1, 9, 10 or 9a, 1, 10, 11 (Figure 1).

Table 4.[a] cos θ and Torsion Angle Values Correlated with Biological Activity (pK_i) and Corresponding Regression Equation

$$pK_iD_1 = 6.292 - 2.70 \cos\theta + 0.025\tau$$

$$R = 0.957, R^2 = 0.916, p = 0.0001, F = 43.575, s = 0.525$$

compd	cos θ	torsion angle (τ)	pK_iD_1 exp	pK_iD_1 calc
1*	−0.05	124.1	9.37	9.52
2*	−0.02	64.4	8.08	7.96
3	0.12	64.4	<5.00	7.50
4	0.26	64.2	<5.00	7.19
5*	0.27	64.1	6.73	7.15
6*	−.01	58.2	8.18	7.77
7*	0.15	55.3	6.85	7.28
8*	0.46	68.4	6.75	6.75
9*	−0.05	11.7	6.38	6.72
10*	0.26	11.5	5.86	5.85
11*	0.24	30.2	6.55	6.37
12*	0.13	30.0	7.06	6.68
15*	−0.21	3.7	6.85	6.98

[a] An asterisk (*) denotes compounds used in development of regression equation. Biological activity expressed as pK_i ($-\log K_i$ in M), torsion angle = τ(8a, 1, 1, 10 or 9a, 1, 10, 11) (see Figure 1). D_1 potencies determined from competition binding experiments with [^{3}H]-SCH23390.

angle for the accessory phenyl ring as a second descriptor in order to describe more effectively its spacial orientation in a multiple regression analysis. Table 4 indicates the final regression equation developed that incorporates those steric and electronic parameters important for D_1 binding affinity as well as predicted binding affinity values (calc. pK_iD_1). Figure 3 graphically demonstrates the significant correlation (r^2 = 0.914) that exists between the experimental versus the calculated pK_iD_1 values. The pK_iD_1 values are estimated based upon the measured values for the racemates.

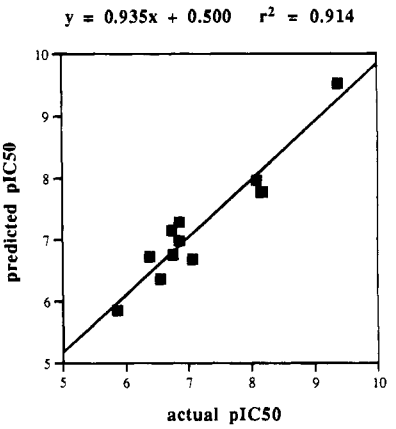

Figure 3. Measured versus predicted D_1 binding affinities.

Comparative Molecular Field Analysis

Comparative molecular field analysis (CoMFA)[27] represents a complementary approach explored in characterizing structural features essential for antagonist binding to the D_1 receptor. CoMFA, a relatively new QSAR technique, attempts to correlate receptor−ligand affinities with the steric and electrostatic fields presented by the ligands thus describing both the electronics and shape. Steric and electrostatic fields of a given set of molecules are sampled at the intersections of a three-dimensional lattice in which they are aligned. Accordingly, one of the most critical steps in developing a successful CoMFA model involves the initial alignment of the molecules within the lattice. Once a suitable alignment has been achieved, independent steric and electrostatic regressor values are generated at each lattice point. These calculated values together with the dependent variable are included in a partial least squares (PLS) analysis utilizing cross-validation for the development of a model with predictive utility

Table 5. Statistical Results from CoMFA Analyses

compd	regressors	alignment	optimal component (S)	cross-validated r^2 (q^2)	press	PLS r^2	s
A	steric electrostatic	RMS[c]	3	0.162	1.070	0.853	0.408
A	steric electrostatic	field fit	4	0.455	1.094	0.993	0.100
A[a]	steric electrostatic torsion angle	field fit	2	0.578	0.727	0.997	0.076
A[b]	steric electrostatic torsion angle	field fit	5	0.698	0.865	0.999	0.057

A = Compounds **1**, **2**, **5**, **6**, **7**, **8**, **9**, **10**, 11, **12**, **13**, and **15**. [a] Compound **13** was omitted from the analysis. [b] Compounds **7** and **13** were omitted from the analysis. [c] RMS = pharmacophoric elements served as reference points for RMS fitting, s = standard error, torsion angle = τ(8a,1,9,10 or 9a,1,10,11)(Figure 1).

for the activities of untested molecules. The cross-validation technique involves random elimination of one or more observations from the original data set with subsequent equation development and activity prediction for the eliminated observation (S) in an iterative manner thus yielding a QSAR equation that is generally of greater predictive value than that derived from conventional regression analysis. Correlations yielding a cross-validated r^2 (q^2) $\geq$ 0.50 are considered to be of predictive utility. The results from the various methods of alignment and regressor combination utilizing the lowest energy conformations of the tetrahydroisoquinolines and the twist-chair conformation of 1 in the development of the final CoMFA model presented are shown in Table 5. Initially, RMS fitting of pharmacophoric elements was used to align the molecules in the region; however, this resulted in an extremely low q^2 value of 0.162. Therefore, the field fit (rigid) alignment option was employed that maximizes steric and electrostatic field overlap as opposed to structural overlap among the members of the data set. Subsequent analyses involving the field fit alignment option of the RMS-fitted molecules still failed to afford a suitably predictive model (q^2 = 0.455) suggesting that perhaps the steric component was still inadequately described as with the original conventional QSAR model.

For these reasons, the corresponding torsion angle values τ(8a,1,9,10 or 9a,1,10,11) weighted equally with the steric and electrostatic regressors were included in the CoMFA model that utilized 11 observations, 2 components, and 11 cross-validation groups to afford a more internally predictive model (q^2 of 0.578). The 1-benzyltetrahydroisoquinoline **13** could not be included in this model since it is not possible to define the corresponding torsion angle. The largest residual resulting from this analysis corresponded to **7**. As a result of elimination of this compound, the analysis afforded a q^2 of 0.698. Non-cross-validation for the former study using two components resulted in a conventional r^2 of 0.997 whereas non-cross-validation for the latter analysis using a five-component model resulted in a r^2 = 0.999. Although **7** differs from the majority of the remaining observations in that this analog possesses no *N*-substituent, the activity of 11 (that also lacks an *N*-substituent) is more adequately predicted. Therefore, it is difficult to justify the elimination of **7** from the data set used to develop the model. Accordingly, the two-component model was used to afford the internally predicted activities correlated with experimental values and for the development of the steric coefficient contour map shown in Figure 4. In Figure 4 the positive steric coefficient contours are depicted indicating that increased steric bulk in these areas should result in enhanced binding affinity. Accordingly, the 6-bromo-7-hydroxy- (**2**), 6-chloro-7-hydroxytetrahydroisoquinolines (**6**) and 1 show favorable steric interaction with the contour regions that accommodate the halogen and *N*-methyl groups whereas analogs that bind weakly (**3**, **4**, **7**, 11, **12**) to the D_1 receptor show reduced interaction. The above inactive analogs lack at least one of the corresponding groups present on the three active analogs that interact with the positive steric contours—namely the 6-substituent on the tetrahydroisoquinolines or the 7-substituent on the tetrahydrobenzazepines or the *N*-methyl group at the nitrogen in the 2- or 3-position of the heterocyclic ring in the tetrahydroisoquinolines and benzazepines, respectively. Increased steric bulk in the areas corresponding to the negative steric coefficient contours (not shown) should result in reduced receptor affinity. The high-affinity analogs 1, **2**, and **6** do not possess groups that protrude into these unfavorable contours. It is evident, however, that of the inactive analogs included, the *N*-propyl group of **8** as well as the less orthogonal accessory phenyl rings of **9** and **10** to protrude into these negative contour regions.

CoMFA has provided an excellent way to evaluate those features important for binding affinity. In order to develop this method, it was necessary to include not only the steric and electrostatic field components but also, as in the case of the conventional QSAR model, an additional steric component, torsion angle of the accessory phenyl ring. While the conventional QSAR approach afforded a suitable correlation, CoMFA offered a better intuitive understanding than purely statistical presentation.

Multifit Analysis: Receptor Mapping

In addition to conventional regression analysis and CoMFA, another approach was taken to characterize the D_1 receptor antagonist model. A multifit analysis was extended relative to our original work.[21] This approach allows for the energy minimization of a set of analogs proposed to interact with the same receptor while constraining the pharmacophoric elements in a similar three-dimensional arrangement as that of an active template. Boolean volumetric representations are subsequently generated that allow for the description of "active space" that is accessible to the ligand and "inactive space" that is partially receptor occupied and not available for ligand binding. The procedure involves linking the above-described pharmacophoric elements by a force constant followed by molecular mechanics-based energy minimization of the conglomerate. Each molecule experiences only the restraining forces of the pharmacophoric template and is unaware of the other superimposed molecules. Subsequent to energy minimization, the energy differences between the lowest energy conformations for each compound (except for the

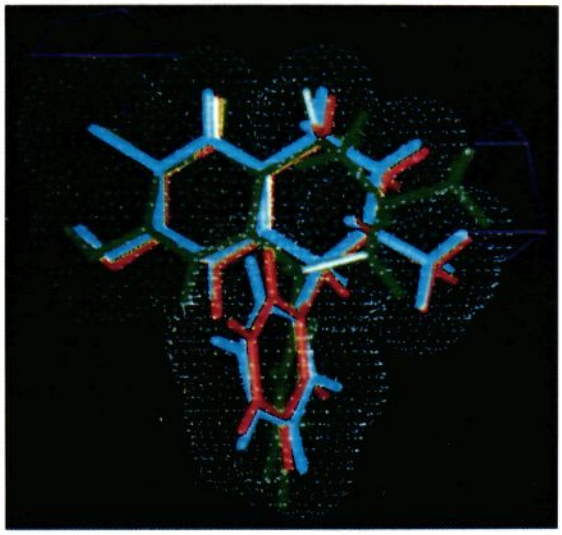

Figure 4. Positive steric coefficient contours containing the active analogs **1** (green), **2** (blue), and **6** (red). Contour regions indicate areas where increased steric bulk should enhance binding. The contour level is 0.01.

Table 6. Energy Differences between Lowest Energy and Multifit Conformations

compd no.	starting energy (kcal/mol)	multifit energy (kcal/mol)	energy difference
1[a]	13.03	21.68	8.65
–2	5.72	7.33	1.61
5	5.88	7.37	1.49
6	5.35	6.39	1.04
7	4.51	5.51	1.00
8	7.80	9.91	2.11
9	12.89	17.25	4.36
10	13.00	16.33	3.33
11	4.75	7.32	2.57
12	5.92	8.32	2.40
13	7.21	23.47	16.26
15	13.42	48.45	35.03

[a] Twist chair conformation used.

twist chair conformation of **1**), and the resulting multifit conformations were determined.

As shown in Table 6, the energy requirement to assume the multifit conformations was less than 4.5 kcal/mol for all analogs except the 1-benzyltetrahydroisoquinoline **13**, the tetrahydrobenzazepine **1**, and the hexahydrobenzophenanthridine **15**. The active space was generated (Figure 5) for those compounds designated as such (**1**, **2**, and **6**). It is notable that the representation of the active space varied little from that previously reported[21] since the only structural feature varied in the additional analog **2** is the size of the halogen substituent in the 6-position. Also, it is reasonable to expect less allowable variation in the active space as compared to the inactive space due to the stringent requirement for critical structural elements of active ligands. Figure 5 represents compounds defined as inactive (**5**, **7**, **8**, **9**, **10**, **11**, **12**, **13**, **15**) contained within the active space. It is evident that elements of the benzyl substituent in **13**, the accessory phenyl ring in the tetrahydrodibenzoquinolizines **9** and **10** and benzophenanthridine **15** and the *N*-propyl substituent of **8** extend beyond the corresponding regions of the active space, further suggesting the importance of the orientation of the accessory phenyl ring, the size and orientation of the *N*-substituent, and orientation of the nitrogen

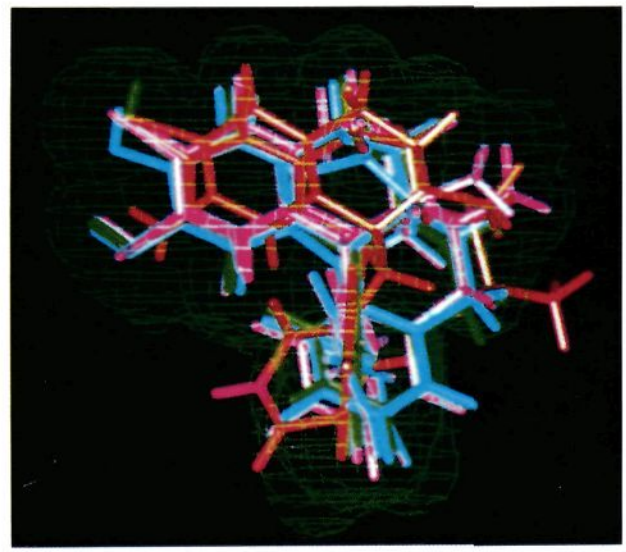

Figure 5. Active space representation containing the inactive analogs **5**, **7**, **8**, **9**, **10**, **11**, **12**, **13**, and **15**.

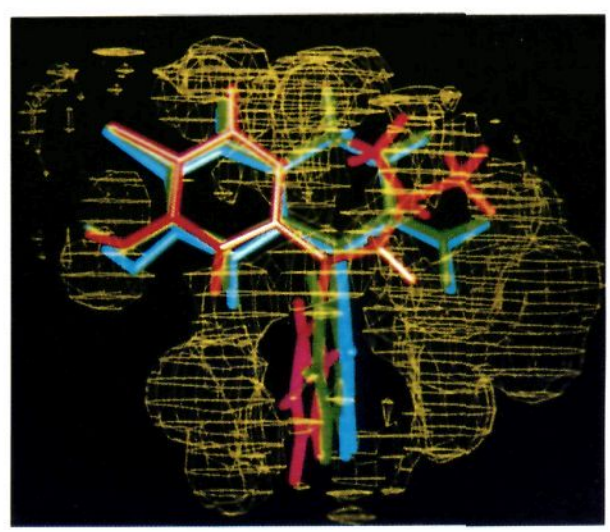

Figure 6. Inactive space representation containing active analogs **1** (red), **2** (blue), and **6** (green).

lone electron pair vector for significant receptor affinity. Figure 6 depicts the inactive space that was generated by subtracting the volume of the active analogs from the total volume affording the peripheral volume that is not accessible for ligand binding. In Figure 6, the active compounds are shown within the inactive space. Most notably, the orthogonal accessory phenyl rings, *N*-substituent methyl groups, and aromatic substituents of these analogs reside within clefts that do not include the inactive space. Compared to the earlier report,[21] additional inactive space is now defined by that volume corresponding to the less orthogonal accessory phenyl rings in the dibenzoquinolizines **9** and **10** as well as the benzophenanthridine **15** (Figure 5). These observations are also in accordance with the critical descriptors used to develop the conventional QSAR. It should be possible to predict qualitatively whether a given molecule should demonstrate binding affinity for the D_1 receptor based upon the alignment of critical structural features within the active and inactive spaces.

In conclusion, our SAR and modeling studies further suggest that both a halogen and hydroxyl in the 6- and

7-positions of the tetrahydroisoquinolines as well as an orthogonal accessory phenyl ring orientation are necessary for D_1 antagonist binding affinity. Both conventional QSAR and CoMFA studies confirm these findings, and the correlations resulting from both techniques are improved by inclusion of the torsion angle of the accessory phenyl ring as an additional regressor.

Experimental Section

All chemicals were used as obtained from the manufacturer. Phenethylamines **16**, **18**, and **19** were obtained from Aldrich Chemical Co. Melting points were recorded on a Mel-Temp melting point apparatus and are uncorrected. ^{1}H-NMR spectra were obtained on a Bruker AC 300 MHz spectrometer using $CDCl_3$ or CD_3OD as solvent. Only one NMR analysis per compound was reported, as the spectra of optical antipodes were virtually identical. Thin-layer chromatography was performed with silica gel 60 coated plates, and column chromatography was performed with silica gel 60 (70–230 mesh). Elemental compositions of novel compounds were determined by Galbraith Laboratories, Knoxville, TN, or MHW Laboratories, Phoenix, AZ, and were correct within ±0.4% of theory. [^{3}H]SCH23390 (79 Ci/mmol) was synthesized by the method of Wyrick *et al.*[32] [^{3}H]Spiperone was purchased from Amersham Corp. (Arlington Heights, IL).

3-Bromo-4-methoxyphenethylamine (17). To a solution of **16** (25.0 g, 0.165 mol) in glacial acetic acid (300 mL) was added a solution of bromine (31.7 g, 0.198 mol) in glacial acetic acid (200 mL) dropwise. A white precipitate formed immediately, and the reaction was stirred at room temperature for 48 h. The white solid was filtered and washed with hexane to obtain the hydrobromide salt. This salt was dissolved in water and adjusted to a pH of 8.0 for the conversion to free base. The suspension was extracted with CH_2Cl_2 and dried (Na_2SO_4), and the volatiles were removed *in vacuo* to afford 25.0 g of **17** (65%): mp 79–80 °C; ^{1}H-NMR ($CDCl_3$) δ 7.40 (d, 1H, Ar*H*$_2$), 7.10 (q, 1H, ArH6), 6.80 (d, 1H, Ar*H*$_5$), 3.88 (s, 3H, OC*H*$_3$), 2.95 (t, 2H, PhC*H*$_2$), 2.7 (t, H, C*H*$_2$N), 1.90 (s, 2H, N*H*$_2$).

N-Benzoylphenethylamines (20–23). General Procedure. To a stirred solution of the phenethylamines **16–19** (0.16 mol) in anhydrous Et_2O under N_2 was added 51.0 mL of 20% NaOH. Freshly distilled benzoyl chloride (19.0 mL, 0.16 mol) was added dropwise with stirring. A white precipitate formed immediately, and the reaction mixture was stirred at room temperature overnight. The colorless solid precipitate was filtered, washed with ether, and dried *in vacuo* to afford a colorless solid (Table 1): ^{1}H-NMR ($CDCl_3$) δ 7.85–6.78 (m, 8H, Ar*H*), 3.88 (s, 3H, OC*H*$_3$), 3.70 (t, 2H, PhC*H*$_2$, 2.8 (t 2H,-C*H*$_2$N).

1-Phenyl-3,4-dihydroisoquinolines (24–27). General Procedure. To a three-neck, round-bottom flask under N_2 containing 0.12 mol of **20–23** in 1044 mL of dry xylenes was added P_2O_5 (39.5 g, 0.25 mol) in portions followed by the dropwise addition of 41.2 mL (0.441 mol) of freshly of distilled $POCl_3$. The mixture was stirred at reflux under N_2 for 6 h followed by cooling to room temperature, and the xylenes were decanted. The solid residue was cooled with an ice bath and cautiously triturated with sufficient 10% NaOH to afford a suspension (pH 8–9). The suspension was extracted with CH_2Cl_2, and the organic extracts dried (Na_2SO_4) and evaporated *in vacuo* to afford the crude product that was either used in the next step or purified by column chromatography: ^{1}H-NMR ($CDCl_3$) δ 7.60–7.30 (m, 6H, Ar*H*), 6.75 (s, 1H ArH8), 3.85 (t, 2H, PhC*H*$_2$), 3.70 (s, 3H, OC*H*$_3$), 2.70 (t, 2H, C*H*$_2$N).

1-Phenyl-1,2,3,4-tetrahydroisoquinolines (28–31). General Procedure. To a three-neck, round-bottom flask equipped with a magnetic stirrer was added a solution of 0.02 mol of the imine (**24–27**), in 128 mL of MeOH containing 1.95 mL of acetic acid under N_2. The solution was cooled to 5 °C, and solid $NaBH_4$ (2.2 g, 0.06 mol) was added in portions. The solution was stirred for 1 h at room temperature, 50 °C for 4 h, and then at room temperature overnight. Water was added, and the mixture was concentrated *in vacuo*. The aqueous suspension was extracted with CH_2Cl_2 and dried (Na_2SO_4), and the volatiles were removed *in vacuo* to afford the crude product that was purified by recrystallization or column chromatography: ^{1}H-NMR ($CDCl_3$) δ 7.10–7.40 (m, 6H, Ar*H*), 6.29 (s, 1H, Ar*H*8), 5.05 (s, 1H, PhC*H*N), 3.65 (s, 3H, OC*H*$_3$), 3.30–2.75 (m, 4H, PhC*H*$_2$C*H*$_2$N).

***N*-Methyl-1-phenyl-1,2,3,4-tetrahydroisoquinolines (32–35). General Procedure.** The tetrahydroisoquinolines **28–31** (7.0 mmol), 37% formaldehyde (9.38 mL), and 14.3 mL of 98% formic acid were stirred at reflux under N_2 for 4 h. The volatiles were removed *in vacuo*, and the residue was adjusted to pH 8.0 with saturated aqueous $NaHCO_3$. The suspension was extracted with CH_2Cl_2, dried (Na_2SO_4), and evaporated *in vacuo* to afford the crude product that was either used crude or purified by recrystallization or column chromatography: ^{1}H-NMR ($CDCl_3$) δ 7.35–7.20 (m, 6H, ArH), 6.15 (s, 1H, Ar*H8*), 4.2 (s, 1H, PhC*H*N), 3.65 (s, 3H, OC*H*$_3$), 3.10–2.90 (m, 2 H, PhCH$_2$C*H*$_2$N), 2.80–2.60 (m, 2H, PhC*H*$_2$), 2.25 (s, 3H NC*H*$_3$).

***N*-Methyl-6-bromo-7-hydroxy- (2), *N*-Methyl-6-hydroxy- (3), and *N*-Methyl-7-hydroxy-1-phenyl-1,2,3,4-tetrahydroisoquinolines (4). General Procedure.** Compounds **32–34** (6.0 mmol) and 66 mL of 48% HBr were heated at 100 °C with stirring for 12 h. The resulting solution was adjusted to pH 8.0 with saturated aqueous $NaHCO_3$ and extracted with CH_2Cl_2. The organic extracts were dried (Na_2SO_4), and the solvent was removed *in vacuo* to afford the crude product that was purified by recrystallization: ^{1}H-NMR ($CDCl_3$) δ 7.10–7.40 (m, 6H, Ar*H*), 6.25 (s, 1H, Ar*H*8), 4.15 (s, 1H, PhC*H*N), 3.30–3.10 (m, 2H, PhCH$_2$), 2.50–2.85 (m, 2H, CH$_2$N), 2.25 (s, 3H NC*H*$_3$).

***N*-Methyl-6,7-dihydroxy-1-phenyl-1,2,3,4-tetrahydroisoquinoline (5).** To a 100-mL three-neck flask equipped with a magnetic stir bar, N_2 inlet, thermometer, and addition funnel was added a solution of the tetrahydoisoquinoline **35** (1.8 mmol) in 46 mL of CH_2Cl_2. This solution was cooled to 0 °C, BBr_3 (5.3 mL, 5.5 mmol) was then added slowly, and this solution was stirred at room temperature for 12 h. To the reaction mixture was added 46 mL of an ice and H_2O mixture that resulted in formation of a white precipitate. The precipitate was filtered, washed with ether, and dried *in vacuo* to afford a colorless solid: ^{1}H-NMR (CD_3OD) δ 7.20–7.40 (m, 5 H, Ar*H*), 6.55 (s, 1 H, Ar*H*5), 6.00 (s, 1 H, Ar*H*8), 4.40 (s, 1H, PhC*H*N), 3.30–3.00 (m, 2H, PhCH$_2$), 2.85–2.70 (m, 2H, CH$_2$N), 2.15 (s, 3H NC*H*$_3$).

***(R)*-(+)-6-Bromo-7-methoxy-1-phenyl-1,2,3,4-tetrahydroisoquinoline ((+)-28).** Racemic **28** (13.3 g, 41.8 mmol) and *N*-acetyl-D-leucine (7.24 g, 41.8 mmol) were dissolved under reflux in CH_3CN (220 mL). Ater the mixture was allowed to sit at room temperature overnight, the white solid was collected and washed with cold CH_3CN followed by Et_2O. The colorless diastereomeric salt mixture was dried *in vacuo* and the specific rotation determined. This process was repeated until a constant rotation of $[\alpha]^{25}_D$ +20.28° was obtained, mp 168–169 °C. The resultant 6.10 g of salt was stirred in 126 mL each of Et_2O and 0.5 N NaOH to obtain the free base. The Et_2O layer was separated, dried (Na_2SO_4), and evaporated *in vacuo* to afford 4.4 g of a colorless solid: mp 101–102 °C; $[\alpha]^{25}_D$ +34.84°.

***(S)*-(−)-6-Bromo-7-methoxy-1-phenyl-1,2,3,4-tetrahydroisoquinoline ((−)-28).** The combined mother liquors from the resolution of (+)-**28** were evaporated *in vacuo*, and the residue was converted to the free base with 300 mL each of Et_2O and 0.5 N NaOH with stirring. The etheral solution was dried (Na_2SO_4) and evaporated *in vacuo* to afford 7.8 g of free base. This solid was refluxed with *N*-acetyl-L-leucine (4.24 g, 24.5 mmol) in 128 mL of CH_3CN for 45 min and allowed to sit at room temperature overnight. The resultant crystals were filtered, washed with cold CH_3CN followed by cold Et_2O, and dried *in vacuo* to give 9.1 g of a colorless solid. This process was repeated until a constant specific rotation of $[\alpha]^{25}_D$ −19.32° was obtained; mp 168–170 °C. This salt was converted to free base by stirring in 146 mL each of 0.5 N NaOH and Et_2O. The Et_2O layer was dried (Na_2SO_4) and evaporated *in vacuo* to give 4.2 g of a colorless solid: mp 101–102 °C; $[\alpha]^{25}_D$ −36.48°.

***(R)*-(−)-*N*-Methyl-6-bromo-7-methoxy-1-phenyl-1,2,3,4-tetrahydroisoquinoline ((−)-32).** Compound (+)-**28** (4.4 g, 13.8 mmol) was *N*-methylated with 98% formic acid (28 mL)

and 37% formaldehyde (18 mL) as described above for racemic **32** to give 3.5 g (76%) of a light yellow gum: $[\alpha]^{25}_D$ −15.09°.

***(S)*-(+)-*N*-Methyl-6-bromo-7-methoxy-1-phenyl-1,2,3,4-tetrahydroisoquinoline ((+)-32).** Compound (−)-**28** (4.2 g, 13.2 mmol) was *N*-methylated with 98% formic acid (26 mL) and 37% formaldehyde (17 mL) as described above for racemic **32** to give 3.8 g (87%) of a light yellow gum: $[\alpha]^{25}_D$ +12.61°.

***(R)*-(−)-*N*-Methyl-6-bromo-7-hydroxy-1-phenyl-1,2,3,4-tetrahydroisoquinoline ((−)-2).** Compound (−)-**32** (3.5 g, 10.5 mmol) was *O*-demethylated with 48% HBr (105 mL) as described above for racemic **2**. The crude product was chromatographted on a column using 10 g of silica gel (CH_2Cl_2−EtOAC, 95:5) to afford a brownish solid that was further purified by recrystallization using CH_2Cl_2 to afford 343 mg (10%) of colorless solid: mp $[\alpha]^{25}_D$ −28.79°; ^{1}H NMR ($CDCl_3$) δ 7.10-7.40 (m, 6H, Ar*H*), 6.25 (s, 1H, Ar*H*8), 4.15 (s, 1H, PhC*H*N), 3.30−3.10 (m, 2H, $PhCH_2$), 2.50−2.85 (m, 2H, CH_2N), 2.25 (s, 3H NCH_3).

***(S)*-(+)-*N*-Methyl-6-bromo-7-hydroxy-1-phenyl-1,2,3,4-tetrahydroisoquinoline ((+)-2).** Compound (+)-**32** (3.8 g, 11.4 mmol) was *O*-demethylated with 48% HBr (114 mL) as described above for racemic **2**. The crude product was chromatographed on a column using 10 g of silica gel (CH_2Cl_2−EtOAC, 95:5) to give a brownish solid that was purified further by repeated recrystallization using CH_2Cl_2 to afford 48 mg (1.3%) of colorless solid: $[\alpha]^{25}_D$ +26.56°.

***N*-(2-Hydroxyethyl)-6-chloro-7-methoxy-1-phenyl-1,2,3,4-tetrahydroisoquinoline (38).** To a solution of **37** (2.5 g, 9.0 mmol) in DMF (71 mL) over K_2CO_3 (1.5 g, 10.0 mmol) was added bromoethanol (1.29 mL, 18.0 mmol) dropwise. This mixture was then heated at 55 °C for 4 h. The DMF was evaporated *in vacuo* and the residue partitioned between H_2O and CH_2Cl_2. The organic layer was separated, dried (Na_2SO_4) and evaporated *in vacuo*. The crude product was purified by column chromatography using 10 g of silica gel (CH_2Cl_2−ether, 95:5) to afford 500 mg (18%) of a yellow gum: ^{1}H-NMR ($CDCl_3$) δ 7.40−7.10 (m, 6H, Ar*H*), 6.25 (s, 1H, Ar*H*8), 4.15 (s, 1H, PhC*H*N), 3.80−3.60 (m, 2 H, $PhCH_2$), 3.65 (s, 3H, OCH_3), 3.40−3.10 (m, 2 H, CH_2N), 3.30−2.60 (m, 4H NCH_2CH_2OH), 2.0 (br s, 1H, O*H*).

3-Chloro-2-hydroxy-5,6,8,9-tetrahydro-13b*H*-dibenzo[*a*,*h*]quinolizine (9). Polyphosphoric acid (PPA) (15 g) was added to **38** (1 mmol), and this mixture was heated at 150 °C for 6 h with stirring. Ice (10 g) was added slowly to the reaction mixture. The resulting aqueous mixture was extracted with ether and adjusted to pH 7 with $NaHCO_3$. The alkaline suspension was extracted with CH_2Cl_2, and the organic extracts were dried (Na_2SO_4) and evaporated *in vacuo* to afford a brown solid. Recrystallization from EtOAC afforded 10 mg (2%) of a light tan solid: mp 225−226 °C; ^{1}H NMR (DMSO-d_6) δ 7.20−7.05 (m, 5H, Ar*H*), 6.67 (s, 1H, Ar*H*8), 4.40 (s, 1H, PhC*H*N), 3.40−2.60 (m, 8H, $PhCH_2CH_2NCH_2CH_2Ph$). Anal. ($C_{17}H_{15}ClNO$) C, H.

2,3-Dihydroxy-5,6,8,9-tetrahydro-13b*H*-dibenzo[*a*,*h*]quinolizine (10). Compound **36**[31] (1.66 g, 5.56 mmol) and 48% HBr (56 mL) were stirred at reflux under N_2 for 4 h at which time the HBr was evaporated *in vacuo*. The resulting product was recrystallized from ethanol to yield 900 mg (46%) of a white solid: mp 261−263 °C; ^{1}H NMR ($CDCl_3$) δ 7.45−7.25 (m, 5H, Ar*H*), 6.70 (s, 1H, Ar*H*5), 6.55 (s, 1H, Ar*H*8) 5.15 (s, 1H, PhC*H*N), 3.80−3.00 (m, 8 H, $PhCH_2CH_2NCH_2CH_2Ph$). Anal. ($C_{17}H_{18}NO_2$) C,H.

Assignment of Absolute Configuration. (*R*)-(−)-*N*-Methyl-6-chloro-7-hydroxy-1-phenyl-1,2,3,4-tetrahydroisoquinoline[20] *(R)*-(−)-**6** and (−)-**2** were both converted to (*R*)-(−)-**4** by catalytic hydrogenolysis. (*R*)-(−)-*N*-Methyl-6-bromo-7-hydroxy-1-phenyl-1,2,3,4-tetrahydroisoquinoline ((−)-**2**) (100 mg, 0.36 mmol) in dry THF (30 mL) containing 0.5 mL of triethylamine and 50 mg of Pd/C was shaken on a Parr apparatus at room temperature under 45 psi of hydrogen for 12 h. The resulting mixture was filtered through Celite to remove the catalyst. Solvent was then removed from the filtrate *in vacuo*, and the crude product was purified by chromatography using 1 g of silica gel (CH_2Cl_2−MeOH, 95:5) to afford 30 mg (40%) of a colorless solid: mp 190−191 °C; $[\alpha]^{25}_D$ −34.84°; ^{1}H NMR ($CDCl_3$) δ 7.40−7.10 (m, 5H, Ar*H*), 6.95 (d, 1H, Ar*H*5), 6.55 (d, 1H, Ar*H*6), 6.00 (s, 1H, Ar*H*8), 4.25 (s, 1 H, PhC*H*N), 3.33−3.10 (m, 2H, $PhCH_2$), 2.85−2.55 (m, 2H, CH_2N), 2.20 (s, 3H, CH_3).

(*R*)-(−)-*N*-Methyl-6-chloro-7-hydroxy-1-phenyl-1,2,3,4-tetrahydroisoquinoline (*(R)*-(−)-**6**) was converted to the dehalogenated product (*R*)-(−)-**4** and purified in the same manner as indicated for (−)-**2**. The final product (75 mg, 85%) was a colorless solid: mp 187−188 °C; $[A]^{25}_D$ −28.20°.

Radioreceptor Assays. Adult male Sprague−Dawley rats were sacrificed by decapitation and the brains dissected rapidly on ice.[33] The corpus striatum of the animals was removed, frozen immediately on dry ice, and either used fresh or stored at −80 °C until used in binding studies. Striatal tissue was homogenized in 50 mM HEPES buffer (pH 7.4, 25 °C) at a Brinkman Polytron PCU-2 setting of 3.0 for 5 s. The tissue suspension was then centrifuged at 32000*g* for 15 min, the supernatant discarded, and this wash step repeated. After the second wash the final pellet was resuspended at a wet weight concentration of 1.25 mg of tissue/mL of buffer for use. Radioligand binding was performed in 12 × 75 mm culture tubes at a total assay volume fo 1.0 mL. Each tube contained 100 μL of competitor, 100 μL of radioligand, and 800 μL of tissue homogenate prepared as described above. Competing drugs were dissolved in 0.1% tartaric acid at 1.0 mM concentrations and diluted appropriately with buffer. [^{3}H]SCH23390 and [^{3}H]spiperone, at 0.25 and 0.02 nM concentrations, respectively, were diluted from methanol stock solutions with buffer. All tubes in the spiperone assays also contained a final concentration of 50 nM ketanserin in order to mask 5-HT_2 receptor binding. Chlorpromazine was used to define nonspecific binding in both cases. Reactions were initiated by the addition of tissue to tubes already containing radioligand and any competitors. The tubes, maintained on ice prior to the addition of tissue, were then vortexed and incubated at 37 °C for 15 min. Binding was terminated by rapid filtration over 1 μm glass fiber filters onto a Skatron cell harvester. IC50 values were calculated from a linear regression of a Hill transformation with all n_H values equal to 1 ± 0.1 for these compounds. Therefore, K_i values were calculated on the basis of the Cheng-Prusoff relationship for competitive inhibition.

Computer-Assisted Conformational Analysis and Molecular Modeling Methods. Molecular mechanics calculations were performed on the 1-phenyltetrahydroisoquinolines and 5,6,8,9-tetrahydro-13b*H*-dibenzoquinolizines reported herein using MM2(87),[34] which contains both MM2 for nonconjugated systems and MMP2 for conjugated π or aromatic systems, on a VAX6330 mainframe computer as described previously.[21] The conformational analysis for the benzophenanthridines has been previously reported.[26]

Utilizing input geometries of the ammonium cations followed by initial geometry optimization using Maximin2 with an energy difference of 0.001 kcal/mol in SYBYL 5.4,[35] the resulting conformations were transferred to MM2(87) via MODEL 2.91 file conversion in order to characterize fully the energy surface for each analog as well as to calculate the dipole moment vector coordinates to be used in the conventional QSAR study described below. As described previously,[21] four different heterocyclic ring half-chair and four boat conformations for the tetrahydroisoquinolines were explored followed by energy minimization in MM2(87). Subsequently, torsion angle τ(a,b,c,d) was driven through 360° in 10-deg increments with the Dihedral Driver function using the lowest energy ring conformation found for each analog. The four lowest energy conformations for the dibenzoquinolizines **9** and **10** (Figure 3) were generated via the Randomsearch routine in Sybyl 5.4. In doing so, all nonaromatic ring bonds were searched. The resulting conformations were subsequently transferred into MM2(87) as described above.

Once the global minimum energy conformations had been calculated for each analog, the MM2(87) atomic coordinate files were transferred into Sybyl 5.4. Next, Sybyl Multifit analysis was performed using the twist-chair conformation of **1** as a template to which the *S* enantiomers of compounds **1**, **2**, **5**, **6**, **7**, **8**, **9**, **10**, **11**, **12**, **13**, and **15** were fitted keeping the chlorines, oxygens, nitrogens, and 1-phenyl centroids linked by a 20

mdynes/Å spring force constant. The results of the Multifit analysis were attained with each molecule having a geometry that ensured conformational similarity of the pharmacophoric elements. The energy difference between these resulting conformations compared to the corresponding starting conformations were determined. Volume calculations were then performed by employing the Mvolume subroutine within Sybyl and defining *(S)*-**2**, *(S)*-**6** and **1** as the active compounds and the *S* enantiomers of **5**, **9**, **10**, **7**, **8**, **11**, **12**, **13**, and **15** as the inactive compounds. Active pharmacophore space accommodated by the receptor was determined by application of the Mvolume addition algorithm to *(S)*-**2**, *(S)*-**6**, and **1**. Inactive substituent space was determined by the volumes of **1**, **2**, **5**, **6**, **7**, **8**, **9**, **10**, **11**, **12**, **13**, and **15** minus the additive volumes of *(S)*-**2**, *(S)*-**6**, and **1** since the inactive compounds also contain certain structural features common to the active compounds.

Determination of Dipole Orientation and Development of a Quantitative Structure–Activity Relationship. As previously described,[21] the energy-optimized final atomic coordinates from the molecular mechanics calculations using MM2(87) were translated so that the center of mass was placed at the origin of the coordinate system and transferred back into Sybyl 5.4. The calculated dipole moment vector from MM2(87) was added to the Sybyl graphics display for each molecule. This vector was extended through the center of mass to the least squares-generated plane of the proposed pharmacophore defined by the Cl, O, N, and 1-phenyl or 1-benzyl centroids. A normal was also constructed through this pharmacophoric plane at the center of mass. The angle θ between the dipole vector and the normal to the plane of the proposed pharmacophore was measured for each molecule, and its cosine was calculated. An additional regressor was defined as the torsion angle τ(a,b,c,d) (Figure 1). The cos θ values and torsion angles were evaluated in a multiple regression analysis versus the D_1 binding potency of the test compounds expressed as the -log K_i using the statistical software STATVIEW 512.[36] Because all analogs except 1, **2**, and **6** were racemates, the K_I values for the *S* enantiomers were estimated as half of the racemate value.

Comparative Molecular Field Analysis (CoMFA). CoMFA analyses were performed using the QSAR option of SYBYL 5.4.

Alignment Rules. Using the lowest energy conformations for compounds **2**, **5**, **6**, **7**, **8**, **9**, **10**, 11, **12**, and **15** and the twist-chair conformation of **1**, the atomic charges for these structures were calculated using the Del Re method. Initially, these compounds were RMS fitted to the template 1 using the pharmacophoric elements designated above as reference points. This method was followed by the Field Fit (rigid) alignment procedure using 1 as the template.

CoMFA Regressor Values. Steric and electrostatic field values were calculated based upon van der Waals (**6-12**) interactions, and electrostatic (Coulombic with a distance-dependent dielectric) potential energy fields. In order to measure these values, a three-dimensional grid extending 2.0 Å along the *x*, *y*, and *z* axes was constructed around all of the molecules in a minimized force field. The steric and electrostatic fields were then calculated at each lattice intersection around the molecules utilizing the Tripos force field based upon the interaction with a probe atom (sp^3 carbon, charge +1). Calculated steric and electrostatic values served as regressors for the partial least squares analysis to explore a possible correlation between these values and biological activity. A subsequent analysis involved the use of the torsion angle described above as an additional regressor weighted equally with the steric and electrostatic values. Partial least squares analyses was carried out with the optimal number of components equal to two and "leave-one-out" cross-validation. The optimal number of components from this analysis was used in the final analysis with zero cross-validation groups for the construction of the coefficient contour plots.

Acknowledgment. This work was supported by PHS Grants MH40537 and MH42705, Center Grants HD03310 and MH33127, and Training Grant GM07040.

References

(1) Carlsson, A. Perspectives on the discovery of central monoaminergic neurotransmission. *Annu. Rev. Neurosci.* **1987**, *10*, 19–40.
(2) Garau, L.; Govoni, S.; Stefanini, E.; Trabucchi, M.; Spano, P. F. Dopamine receptors: pharmacological and anatomical evidences indicate that two distinct dopamine receptor populations are present in rat striatum. *Life Sci.* **1978**, *23*, 1745–1750.
(3) Kebabian, J.; Calne, D. Multiple Receptors for Dopamine. *Nature* **1979**, *277*, 93–96.
(4) Creese, I.; Leff, S. Dopamine Receptors: A Classification. *J. Clin. Psychopharmacol.* **1982**, *2*, 329–335.
(5) Snyder, S. The Dopamine Hypothesis of Schizophrenia: Focus on the Dopamine Receptor. *Am. J. Psychiatry* **1976**, *133*, 197–202.
(6) Lauduron, P. Commentary: Dopamine-sensitive Adenylate Cyclase as a Receptor Site. In *Dopamine Receptors*; Kaiser, C., Kebabian, J., Eds.; American Chemical Society: Washington, D.C., 1983, p 22.
(7) Iorio, L. C.; Barnett, A.; Leitz, F. H.; Houser, V. P.; Korduba, C. SCH23390, A Potential Benzazepine Antipsychotic with Unique Interactions on Dopaminergic Systems. *J. Pharmacol. Exp. Ther.* **1983**, *226*, 462–468.
(8) Mailman, R. B.; Schulz, D. W.; Lewis, M. H.; Staples, L.; Rollema, H.; DeHaven, D. L. SCH-23390: a selective D_1 dopamine antagonist with potent D_2 behavioral actions. *Eur. J. Pharmacol.* **1984**, *101*, 159–160.
(9) Christensen, A. V.; Arnst, J.; Hyttel, J.; Larsen, J. J.; Svendsen, O. Pharmacological effects of a specific dopamine D-1 antagonist SCH 23390 in comparison with neuroleptics. *Life Sci.* **1984**, *34*, 1529–1540.
(10) Clark, D.; White, F. J.; Review: D_1 dopamine receptor – The Search for a Function: A critical evaluation of the D_1/D_2 dopamine receptor classification and its functional implications. *Synapse* **1987**, *1*, 347–388.
(11) Robertson, H. A. Dopamine receptor interactions: some implications for the treatment of Parkinson's disease. *Trends Neurosci.* **1992**, *15*, 201–206.
(12) Anderson, J.; Gingrich, J.; Bates, M.; Dearry, A.; Faladeau, P.; Senogles, S.; Caron, M. Dopamine Receptor Subtypes: Beyond the D_1/D_2 Classification. *Trends Pharmacol. Sci.* **1990**, *22*, 231–236.
(13) Zhou, Q.-Y.; Grandy, D.; Thambi, L.; Kushner, J.; Van Tol, H.; Cone, R.; Pribnow, D.; Salon, J.; Bunzow, J.; Civelli, O. Cloning and Expression of Human and Rat D_1 Dopamine Receptors. *Nature* **1990**, *347*, 76–80.
(14) Dearry, A.; Gingrich, J. A.; Falardeau, P.; Fremeau, R. T.; Bates, M. D.; Caron, M. G. Molecular cloning and expression of the gene for a human D_1 dopamine receptor. *Nature* **1990**, *347*, 72–76.
(15) Sunahara, R.; Niznik, H.; Weiner, D.; Stormann, T.; Brahn, M.; Kennedy, J.; Gelernter, J.; Yang, R.; Israel, Y.; Seeman, P.; O'Dowd, B. Human Dopamine D_1 Receptor Encoded by an Intronless Gene on Chromosome 5. *Nature* **1990**, *347*, 80–83.
(16) Monsma, F. J.; Mahan, L. C.; McVittie, L. D.; Gerfen, C. R.; Sibley. D. R. Molecular cloning and expression of a D_1 dopamine receptor linked to adenylyl cyclase activation. *Proc. Natl. Acad. Sci. U.S.A.* **1990**, *87*, 6723–6727.
(17) Sunahara, R. K.; Gaun, H.-C.; O'Dowd, B. F.; Seeman, P.; Laurier, L. G.; Ng, G.; George, S. R.; Torichia, J.; Van Tol, H. H. M.; Niznik, H. B. Cloning of the gene for a human dopamine D_5 receptor with higher affinity for dopamine than D_1. *Nature* **1991**, *350*, 614–619.
(18) Tiberi, M.; Jarvie, K. R.; Silvia, C.; Falardeau, P.; Gingrich, J. A.; Godinot, N.; Bertrand, L.; Yang-Fang, T. L.; Fremeau, R. T.; Caron, M. G. Cloning, molecular characterization and chromosomal assignment of a gene encoding a second D_1 dopamine receptor subtype: differential expression pattern in rat brain compared with the D_{1A} receptor. *Proc. Natl. Acad. Sci. U.S.A.* **1991**, *88*, 7491–7495.
(19) Taylor, J. R.; Lawrence, M. S.; Redmond, D. E., Jr.; Elsworth, J. D.; Roth, R. H.; Nichols, D. E.; Mailman, R. B. Dihydrexidine, a full dopamine D_1 agonist, reduces MPTP-induced parkinsonism in monkeys. *Eur. J. Pharmacol.* **1991**, *199*, 389–391.
(20) Charifson, P. S.; Wyrick, S. D.; Hoffman, A. J.; Simmons, R. M.; Bowen, J. P.; McDouglad, D. L.; Mailman, R. B. Synthesis and Pharmacological Characterization of 1-Phenyl-, 4-Phenyl-, and 1-Benzyl-1,2,3,4-tetrahydroisoquinolines as Dopamine receptor ligands. *J. Med. Chem.* **1988**, *31*, 1941–1946.
(21) Charifson, P.; Wyrick, S.; Hoffman, A.; Simmons, R.; Bowen, J.; McDouglad, D.; Mailman, R. Conformational Analysis and Molecular Modeling of 1-Phenyl-, 4-Phenyl-, and 1-Benzyl-1,2,3,4-tetrahydroisoquinolines as D_1 Dopamine Receptor Ligands. *J. Med. Chem.* **1988**, *31*, 2050–2058.
(22) Pettersson, I.; Liljefors, T.; Bogeso, K. Conformational Analysis and Structure-activity Relationships of Selective Dopamine D_1

Receptor Agonists and Antagonists of the Benzazepine Series. *J. Med. Chem.* **1990**, *33*, 2197–2204.
(23) Pettersson, I.; Gundertofte, K.; Palm, J.; Liljefors, T. A Study on the Contribution of the 1-Phenyl Substituent to the Molecular Electrostatic Potentials of Some Benzazepines in Relation to Selective Dopamine D_1 Receptor Activity. *J. Med. Chem.* **1992**, *35*, 502–507.
(24) Weinstock, J.; Oh, H. J.; DeBrosse, C. W.; Eggleston, D. S.; Wise, M.; Flaim, K. E.; Gessner, G. W.; Sawyer, J. L.; Kaiser, C. Synthesis, Conformation and Dopaminergic Activity of 5,6-Ethano-bridged Derivatives of Selective Dopaminergic 3-Benzazepines. *J. Med. Chem.* **1987**, *30*, 1303–1308.
(25) Mottola, D. M.; Brewster, W. K.; Cook, L. L.; Nichols, D. E.; Mailman, R. B. Dihydrexidine, A Novel Full Efficacy D_1 Dopamine Receptor Agonist. *J. Pharmacol. Exp. Ther.* **1992**, *262*, 383–393.
(26) Mottola, D. M.; Laiter, S.; Watts, V. J.; Tropsha, A.; Wyrick, S. D.; Nichols, D. E.; Mailman, R. B. Conformational Analysis of D_1 Dopamine Receptor Agonists: Pharmacophore Assessment and Receptor Mapping. *Mol. Pharmacol.* Submitted.
(27) Cramer, R.; Patterson, D.; Bunce, J. D. Comparative Molecular Field Analysis (CoMFA). 1. Effect of Shape on Binding of Steroids to Carrier Proteins. *J. Am. Chem. Soc.* **1988**, *110*, 5959–5967.
(28) Fodor, G.; Gal, J.; Phillips, B. A. The Mechanism of the Bischler-Napieralski Reaction. *Angew. Chem., Int. Ed. Engl.* **1972**, *11*, 919–920.
(29) Clarke, H. T.; Gillespie, H. B.; Weisshaus, S. Z. Methylation of Primary or Secondary Amines with Formaldehyde and Formic Acid: A Special Form of the Leuckart-Wallach Reaction. *J. Am. Chem. Soc.* **1933**, *55*, 4571–4587.
(30) Gold, E. H.; Chang, W. K. U.S. Patent 4349472, Sept 14, 1982.
(31) Vlaeminck, F.; DeCock, E.; Tourwe, D.; Van Binst, G. Synthesis and Conformation of 5,6,8,9-tetrahydro-13bH-dibenΣ[a,h]quinolizine and 5,6,8,9,14,14b-hexahydrobenzo[a]indolo[3,2-h]quinolizine. *Heterocycles* **1981**, *15*, 1213–1218.
(32) Wyrick, S. D.; McDouglad, D. L.; Mailman, R. B. Multiple Tritium Labelling of (+)-7-Chloro-8-hydroxy-1-phenyl-3-methyl-2,3,4,5-tetrahydro-1H-3-benzazepine, SCH23390. *J. Lab. Compd. Radiopharm.* **1986**, *23*, 685–692.
(33) Schulz, D. W.; Staples, L. J.; Mailman, R. B. SCH23390 Causes Persistant Antidopaminergic Effects *in vivo*: Evidence for Long Term Occupation of Receptors. *Life Sci.* **1985**, *36*, 1941–1948.
(34) Allinger, N.; et al. MM2(87) software, Molecular Design, Ltd.
(35) SYBYL Version 5.4, Tripos and Associates, St. Louis, MO, 1991.
(36) StatView 512+ software package, Brain Power Inc., Calabasas, CA, 1986.